J Neurophysiol 92: 1023–1033, 2004.
First published April 7, 2004; 10.1152/jn.01089.2003.

Impact of Noise on Retinal Coding of Visual Signals

Christopher L. Passaglia[1,2] and John B. Troy[1]

[1]*Biomedical Engineering Department and Neuroscience Institute, Northwestern University, Evanston, Illinois 60208; and* [2]*Biomedical Engineering Department, Boston University, Boston, Massachusetts 02215*

Submitted 10 November 2003; accepted in final form 31 March 2004

Passaglia, Christopher L. and John B. Troy. Impact of noise on retinal coding of visual signals. *J Neurophysiol* 92: 1023–1033, 2004. First published April 7, 2004; 10.1152/jn.01089.2003. Neural noise introduces uncertainty about the signals encoded in neural spike trains. Because of the uncertainty neurons can reliably transmit a limited amount of information. This amount is difficult to quantify for neurons that combine signals and noise in a complex manner, as many trials would be needed to estimate the joint probability distribution of stimulus and neural response accurately. The task is experimentally tractable, however, for neurons that combine signals with additive Gaussian noise. For such neurons, the joint probability distribution is well defined and information transmission rates can be computed from estimates of signal-to-noise ratio. Here we use power spectral analysis to specify the contributions of signal and noise to retinal coding of visual information. We show that in the spike trains of cat ganglion cells noise power is minimal and constant at temporal frequencies from 0.3 to 20 Hz and that it increases at higher frequencies to a plateau level that generally depends on stimulus contrast. We also show that trial-to-trial fluctuations in noise amplitude at different frequencies are uncorrelated and normally distributed. Although the contrast dependence indicates that noise at high temporal frequencies contributes nonlinearly to ganglion cell spike trains, cells in the primary visual cortex are not known to respond to stimulus modulations >20 Hz. Hence, noise in the retinal output would appear additive, white, and Gaussian from their perspective. This greatly simplifies analysis of information transmission from the eye to the primary visual cortex and perhaps other regions of the brain.

INTRODUCTION

Most neurons communicate with action potentials. The timing of these action potentials is erratic due to the signal being transmitted and to noise that accompanies it. When the transmitted signal can be reliably distinguished from spike discharge noise, information flows from one neuron to the next. Distinguishing signal from noise in a world that is forever changing requires knowledge about the statistical properties of neural responses and their representation of sensory input. How neurons obtain this knowledge is uncertain but analyses of their spike trains have provided much insight into what neurons might learn.

In the mammalian retina, it is known that most ganglion cells randomly discharge spikes at a moderate rate even in darkness and that the characteristics of this maintained discharge vary with illumination level (Barlow and Levick 1969; Kuffler et al. 1957; Rodieck 1967). Some of the discharge noise can be attributed to the stochastic nature of light (Hecht et al. 1942). The rest originates from within the retina. At low light levels, the main source of noise in the retinal output lies in the spurious isomerizations of rhodopsin molecules in rod photoreceptors, which trigger ganglion cells to fire bursts of spikes (Barlow et al. 1971). At higher light levels, adaptation sets in and ganglion cells cease to burst. In this regime, the origin of the maintained discharge is less clear. It could derive from transduction noise in cone photoreceptors (Schneeweis and Schnapf 1999; Shapley and Enroth-Cugell 1984). Or it could arise later along the retinal pathway during synaptic transmission (Freed 2000; Frishman and Levine 1983; van Rossum et al. 2003) or spike generation (Croner et al. 1993; Schellart and Spekreijse 1973; van Dijk and Ringo 1987; van Rossum et al. 2003).

Because visual perception is ultimately limited by the noise in ganglion cell spike trains, the statistical properties of the maintained discharge have been carefully analyzed at various light levels. Under photopic illumination, which is the realm of this paper, the discharge behaves like a renewal process with gamma-distributed interspike intervals to a good approximation (Kuffler et al. 1957; Troy and Robson 1992). Such a process is completely defined by the mean interval and the SD of intervals, and studies have shown that these two discharge statistics are positively correlated (Frishman and Levine 1983; Troy and Robson 1992), meaning that ganglion cells with high discharge rates have more regular looking spike trains. Interestingly, when the temporal structure of the maintained discharge was examined, it was found that the dependence of noise variance on mean interspike interval did not hold at all temporal frequencies. Below ~10 Hz the maintained discharge noise was largely independent of spike rate (Troy and Lee 1994; Troy and Robson 1992). This suggests that when ganglion cells are driven by a dynamic stimulus, signal and noise might sum at certain temporal frequencies.

That noise in the retinal output could be additive runs counter to the view of spikes as all-or-nothing events. After all, neural spiking mechanisms are highly nonlinear devices that exhibit refractoriness and firing thresholds. When the retinal signal engages these nonlinearities, the noise accompanying the signal should get transformed as well. For such reasons, it has been argued that spike discharge noise must be multiplicative (Cecchi et al. 2000). Nevertheless, measurements of ganglion cell responses to periodic stimulation have consistently shown the variance in response amplitude to be independent of stimulus strength (Croner et al. 1993; Levine 1994; Rüttiger et al. 2002; van Dijk and Ringo 1987). The impact of noise on retinal information transmission thus remains unclear.

Here we examine how signals and noise combine across temporal frequency to produce the driven discharge of cat

Address for reprint requests and other correspondence: C. L. Passaglia, Boston University, Biomedical Engineering Department, 44 Cummington St., Boston, MA 02215 (E-mail: psagls@bu.edu).

The costs of publication of this article were defrayed in part by the payment of page charges. The article must therefore be hereby marked "*advertisement*" in accordance with 18 U.S.C. Section 1734 solely to indicate this fact.

retinal ganglion cells. We use a spectral representation of the cells' discharge because it provides a convenient measure of the variance in spike rate over different time scales (i.e., temporal frequencies) of the response. By presenting a broadband visual stimulus, we could then quantify the contribution of each frequency component of the signal and noise to ganglion cell spike trains over the entire signaling range of the cells. We find that noise in the retinal output behaves additively or multiplicatively depending on the time scale of interest.

METHODS

Physiological preparation

Anesthesia was induced in adult male cats with sodium pentothal (20 mg/kg iv, supplemented as needed) or occasionally with ketamine HCl mixed with acepromazine (25 and 1 mg/kg im, respectively). Anesthesia was maintained for the duration of the experiment via a steady infusion of ethyl carbamate (15–50 $mg \cdot kg^{-1} \cdot h^{-1}$). Paralysis was achieved via a steady infusion of pancuronium bromide (0.2 $mg \cdot kg^{-1} \cdot h^{-1}$). Paralyzed animals were artificially ventilated and their blood pressure and heart rate continuously monitored to titrate infusion rates. Body temperature and end-tidal CO_2 were also tracked and kept at normal levels. Pupils were dilated with topical application of 1% atropine sulfate and nictitating membranes were retracted with 10% phenylephrine. Eyes were fitted with artificial pupils (4–5 mm diam), and the stimulus was focused onto the retina with auxiliary lenses. All experimental procedures were approved by the Northwestern University Animal Care and Use Committee and were in accordance with the National Institutes of Health guidelines.

Recording and visual stimulation

A craniotomy was performed over the optic tract and a tungsten-in-glass microelectrode was advanced downward through a protective guide tube into the brain. After isolating the spike discharges of a single optic-tract fiber, the receptive field center of the recorded ganglion cell was mapped on a tangent screen onto which the optic disk and major blood vessels surrounding the area centralis of each eye were drawn. These maps were used to estimate retinal eccentricities. The receptive field was then centered via a rotatable mirror onto the display of a video monitor (Multiscan 17se, Sony) running at a frame rate of 150 Hz. The mean luminance (L_{mean}) of the display was 30 cd/m^2, which produced a retinal illuminance (~500 cat trolands for a 4-mm pupil) in the low photopic range of the cat. Custom software controlled the display output and recorded times of spike discharge with 0.1-ms precision via pattern generation (VSG2/2, Cambridge Research Systems) and data-acquisition cards (AS1, Cambridge Research Systems). A battery of tests were performed with the display, such as the null test with contrast reversing gratings (Hochstein and Shapley 1976), which identified the cell as an X, Y, or other ganglion cell type.

Stimulus paradigm

Cells were visually stimulated by randomly assigning the luminance of a central spot on the display one of two values (L_+,L_-) each video frame (Fig. 1*A*). The two values were specified by the equation $L_\pm = [(100 \pm c)/100]L_{mean}$, where c is the percentage contrast of the random binary sequence. Prior to data collection the spot was matched in diameter to the receptive field center of each cell by determining the smallest spot that gave a near-maximal response power. Such a spot should drive the center while minimally activating the receptive field surround. For the center-matched spot, a 90-s random binary sequence was presented two to six times to a cell for a range of contrast settings (0–100%). The sequence repeated itself every 512 frames (3.14-s),

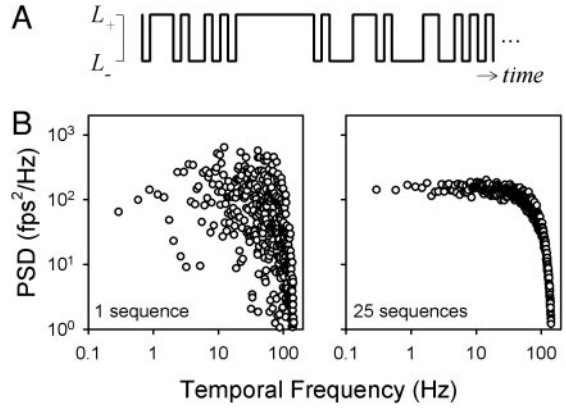

FIG. 1. Temporal characteristics of the visual stimulus. *A*: stimulus waveform presented to cat retinal ganglion cells. The luminance of a spot centered on the receptive field of the cells was randomly assigned the value L_+ or L_- each video frame. The random binary sequence lasted 90 s of which a short segment is shown here. The length of the time arrow corresponds to 2 video frames or ~13.3 ms. *B*: power spectrum of a single random binary sequence (*left*) and the average power spectrum of 25 different random binary sequences (*right*). Stimulus power spectral density is constant up to ~50 Hz on average though for any given random binary sequence it may vary markedly about the average. PSD, power spectral density. fps, frames per sec.

thereby yielding 26 consecutive responses to the same random binary stimulus. The first response to each stimulus presentation was discarded to eliminate transients. For some cells, different 90-s random binary sequences that did not repeat every 512 frames were also presented to the cell. Responses to this stimulus were processed in the same manner as those to the repeated one. Between epochs of data collection, the location of the receptive field on the video monitor was periodically checked to ensure that it remained centered on the spot.

Data analysis

Each of the 50–150 responses to repeated and nonrepeated sequences of a given contrast was expressed as a string of 0's, 1's, and occasional 2's by placing the times of spike discharge into one of 1,024 bins equal in duration to one-half the frame rate (~3.3 ms). Because the repeated sequence should evoke the same response string $r(t)$ in the absence of noise, the mean of the ensemble of strings was considered the signal $x(t)$ encoded in the spike train and the deviation of each string from the ensemble mean was the discharge noise $n(t)$ against which the signal would be detected. That is

$$x(t) = \langle r(t) \rangle$$

$$n(t) = r(t) - \langle r(t) \rangle \quad (1)$$

where brackets denote ensemble averaging. This definition of the encoded signal assumes that noise in the spike train is additive. That is to say, the encoded signal dictates the rate of spike discharge, but the timing of individual spikes is random (i.e., spikes are independent). This is a common assumption in spike train analysis. One could imagine other definitions of the encoded signal, but our results indicate that, to a good approximation, the assumption of additivity is valid over much of the signaling range of ganglion cells. Fourier analysis was subsequently performed on the repeated response, signal, and noise strings and nonrepeated response strings using commercial software (Matlab, The MathWorks). In performing the analysis, the strings were multiplied by 300, the numerical value of the bin rate, so that the Fourier components had units of instantaneous spike rate (imp/s). The scaling factor is necessary because spikes are dimensionless and have arbitrary amplitude. The power spectrum of the signal string $P_X(f)$ and the average power spectrum of the ensemble of response $P_R(f)$ and noise $P_N(f)$ strings were computed as

$$P_X(f) = X(f)X^*(f)\delta f$$

$$P_R(f) = \langle R(f)R^*(f)\delta f\rangle$$

$$P_N(f) = \langle N(f))N^*(f)\delta f\rangle \quad (2)$$

where $R(f)$, $X(f)$, and $N(f)$ are the Fourier transforms of response, signal, and noise strings, asterisks denote the complex conjugate, and δf is the spectral bin width (~0.3 Hz). By summing power spectral densities (except at 0 Hz) and dividing by 300 the variance in ganglion cell spike trains could be measured for any desired band of temporal frequencies.

RESULTS

Reported are results from 11 ON-center X (ON-X) cells, 9 OFF-center X (OFF-X) cells, 9 ON-center Y (ON-Y) cells, and 13 OFF-center Y (OFF-Y) cells whose spike discharges were stable and well isolated for the duration of data collection. Other types of cat retinal ganglion cell were infrequently recorded from the optic tract and not investigated.

Signal and noise in retinal spike trains

Figure 2*A* illustrates the variability of spike discharges of typical ON-X and OFF-X cells under steady uniform photopic illumination. Statistical analyses of spike trains like these have shown that the maintained discharge of retinal ganglion cells is nearly random (Frishman and Levine 1983; Kuffler et al. 1957; Troy and Lee 1994; Troy and Robson 1992). The irregularity of spike discharge for steady illumination contrasts sharply with the orderly pattern of activity evoked by dynamic stimulation. Figure 2*B* displays spike trains collected from the two X cells in response to a small spot centered on their receptive field. The spot was rapidly modulated black and white according to a random binary sequence that was the same on each trial (Fig. 1*A*). A random sequence was used because, for sufficiently high frame rate, this stimulus has power at every temporal frequency to which ganglion cells respond and for each frequency component the power is the same on average (Fig. 1*B*). Responses to this high-contrast broadband stimulus were very reproducible as indicated by mean spike counts of ~1 in several time bins (histograms in Fig. 2*B*). For certain spikes, the jitter in timing was on the order of a few milliseconds (σ = 2–5 ms), consistent with previous measurements (Keat et al. 2001; Reich et al. 1997; Reinagel and Reid 2000). Such precision is widely offered as evidence that the fine patterning of spikes may be important for visual information transmission (Bair and Koch 1996; Berry et al. 1997; de Ruyter van Steveninck et al. 1997; Reich et al. 1997; Reinagel and Reid 2000).

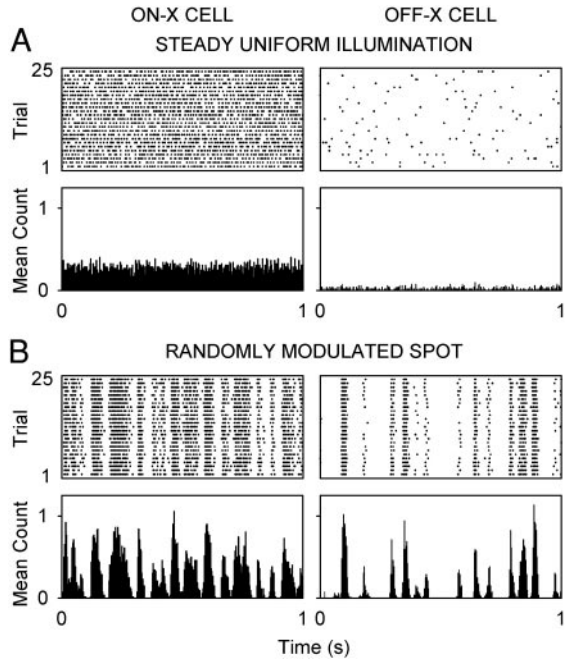

FIG. 2. Variability of firing of retinal ganglion cells during constant and dynamic stimulation. *A*: raster plots (*top*) and histograms (*bottom*) of the spike discharges of an ON-X and OFF-X ganglion cell for steady uniform photopic illumination. The mean firing rate of the ON and OFF cell was 80 and 7 imp/s, respectively. *B*: raster plots and histograms of responses of the same cells to a spot modulated by a random binary sequence of 100% contrast. Shown are 1-s segments of 25 consecutive responses of ~3.4-s duration. For some of the bins, the mean spike count was ~1, indicating a high precision of spiking (i.e., <3.3 ms or 1 bin). The mean firing rate of the ON and OFF cell was 88 and 48 imp/s, respectively.

The high degree of response reproducibility suggests that spike-discharge noise may have decreased when ganglion cells were dynamically driven. To evaluate the suggestion, we extracted the random component of the driven discharge and compared its statistical properties to those of the maintained discharge. Figure 3*A* plots the power spectrum of the maintained discharge of the two X cells and a representative ON-Y and OFF-Y cell. As previously shown for cat and monkey retinal ganglion cells (Troy and Lee 1994; Troy and Robson 1992) and cat lateral geniculate cells (Mukherjee and Kaplan 1998), over the range of 0.3 to 20 Hz noise power spectral density is minimal (i.e., often an order of magnitude less than >20 Hz) and constant and at higher temporal frequencies it plateaus to a value numerically equal to the mean spike rate. A high-frequency plateau was not always evident for OFF cells because some have low maintained discharge rates. It should be noted that at temporal frequencies much below the limits of our analysis (<0.3 Hz) noise power spectral density has been reported to follow a power-law relationship and thus would no longer be constant (Lowen et al. 2001; Teich et al. 1997). Fig. 3*B* (●) plots the average power spectrum of noise in the driven discharge of the four cells over the frequency range of our analysis. The driven discharge noise was extracted by subtracting the average response from individual responses to the randomly modulated spot. Comparison with the maintained discharge spectrum reveals that the effect of visual stimulation on spike discharge noise varied with temporal frequency. For OFF cells, the noise rose markedly at frequencies greater than ~20 Hz due to a stimulus-induced increase in mean spike rate. An increase in high-frequency noise was also seen in some but not all ON cells. Visual stimulation had little or no effect, however, on spike discharge noise at frequencies less than ~20 Hz. This can be demonstrated by subtracting the maintained discharge spectrum from the driven noise spectrum (Fig. 3*C*). Over the range of 0.3–20 Hz, the mean power spectral density of the residual was not significantly different from zero for any of these cells and barely changed for those cells in the ensemble that showed a detectable effect (see Fig. 5). Hence, although dynamic stimuli may elicit reproducible spike trains, the reproducibility does not necessarily translate to less noise in the retinal output.

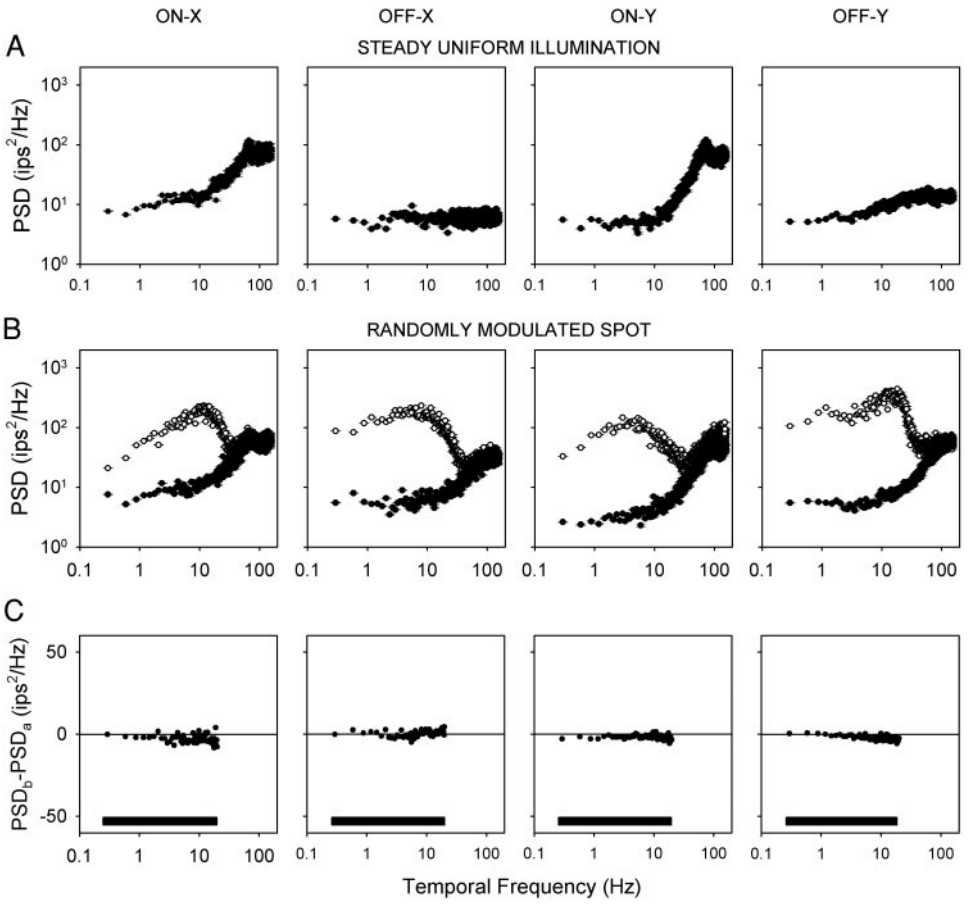

FIG. 3. Spectral analysis of discharge noise during constant and dynamic stimulation. *A*: power spectrum of the maintained discharge of the 2 X cells of Fig. 2 and an ON-Y and OFF-Y cell. Spectra were computed from 100 spike trains during steady uniform illumination. *B*: power spectrum of the responses of the 4 cells to a spot modulated by 100 different random binary sequences (○) and of the driven discharge noise extracted from 100 spot responses to the same random binary sequence (●). Spot contrast was 100%. *C*: difference in power spectral density of the maintained and driven discharge noise over the range of 0.3–20 Hz (bars). Negative frequency components (not shown) have complementary power spectral densities. Error bars give standard errors. PSD, power spectral density.

That the maintained and driven discharge noise spectra were virtually identical for some cells, namely ON-X cells, is a striking and powerful result. It indicates that the contributions of extraneous sources of noise to our measurements, such as eye movements, finite data, or nonstationarity, were negligible. Such noise sources would have the effect of worsening our estimate of the average driven response (i.e., signal) and would ultimately cause the driven discharge noise spectrum to differ from the maintained discharge spectrum. But, this is not what we observed with ON-X cells or, at low temporal frequencies, with other cell types. Even if the average driven response for one-half of the trails was used to specify the noise records for the other half and vice versa, the driven discharge noise spectrum was unaffected ($n = 4$, data not shown). The result was not an artifact of the analysis either. Although spike discharge noise was additive at low temporal frequencies, as the analysis assumes, it was multiplicative at high temporal frequencies for the vast majority of cells.

How could the driven discharge noise be the same or even greater than the maintained discharge noise when the spot responses appear so reliable? Figure 3*B* (○) plots the average power spectrum of the cells' response to a spot modulated each trial by a different random binary sequence. Different sequences were used instead of the same sequence to illustrate a smooth response spectrum (Fig. 1*B*). Comparison with the driven noise spectrum (●) indicates that response power at temporal frequencies >30–50 Hz was due to spike discharge noise because the two spectra superimpose, whereas response power at lower frequencies was due mainly to the encoded signal because the two spectra diverge. This is consistent with previous measurements of the temporal transfer characteristics of the receptive field center of cat ganglion cells at comparable light levels (Frishman et al. 1987). It suggests that the spot responses were reproducible in large part because the stimulus is high in contrast and because noise is minimal and nearly constant over the range of time scales that the stimulus modulates ganglion cell activity. At finer time scales, the noise increases and quickly overwhelms the visual signal, jittering the times of spikes within a burst but generally not across bursts.

Frequency components of noise are independent and Gaussian distributed

That spike discharge noise exhibited constant power spectral density from 0.3 to 20 Hz suggests it may be considered white noise over this frequency range. Such a noise source has frequency components that are independent as well as the same in magnitude. We checked for independence by first examining the trial-to-trial fluctuations in noise amplitude and phase at different temporal frequencies. For white noise, the Fourier components would vary randomly about their mean value, whereas some components should covary if the driven discharge contains correlated noise. Figure 4*A* plots, for a representative cell, the outcome of the analysis using 1, 10, and 100 Hz as a test frequency. Each point in the plot gives the correlation coefficient between the real (ρ_R, ●) or imaginary (ρ_I, ○) noise measurements at the test frequency f_{test} and at frequency f. They were computed from the relationship

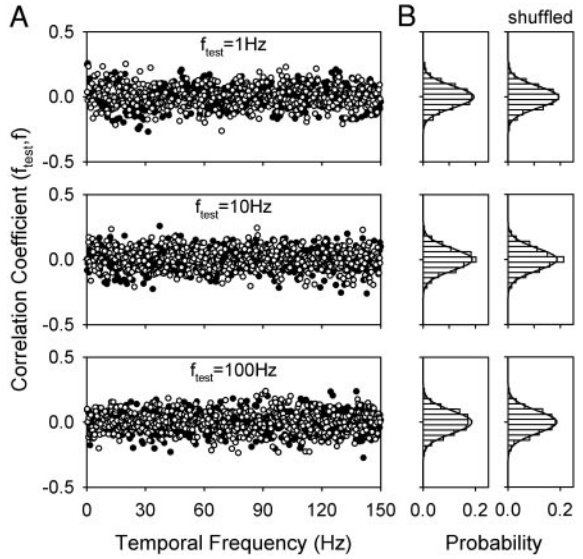

FIG. 4. Frequency components of the driven discharge noise are independent. *A*: correlation coefficient between real (●) and imaginary (○) noise amplitude measurements at 1, 10, and 100 Hz and at other frequencies for an ON-X cell. The coefficient was computed by separately cross-correlating the amplitude of the test frequency f_{test} and that of each other frequency component on a given trial across 150 driven noise records. *B*: histogram of the correlation coefficients in *A* (*left*) and of coefficients computed after shuffling the 150 test frequency measurements (*right*). Because noise fluctuations on different trials would not be correlated, a shuffled histogram gives the distribution of correlation coefficients that is expected by chance. The shuffled and unshuffled histograms were all fit by the same normal probability density function (—), which has a mean of 0 and SD of 0.08. Bin width is 0.04

$$\rho_R = \frac{C_R(f_{test}, f)}{\sqrt{C_R(f_{test}, f_{test})C_R(f,f)}}$$

$$\rho_I = \frac{C_I(f_{test}, f)}{\sqrt{C_I(f_{test}, f_{test})C_I(f, f)}} \quad (3)$$

where C_R and C_I are the covariance of real and imaginary noise measurements. Notice that the correlation coefficients hovered around zero, implying that the Fourier components of noise on one trial were not correlated with those on other trials. Other test frequencies yielded the same result (data not shown). Outlying coefficients were deemed not significant because they varied from cell to cell, they would be expected by chance since real and imaginary coefficients were normally distributed about a mean of zero (Fig. 4*B*, *left*), and correlating noise measurements at f and f_{test} on different trials as opposed to the same trials gave essentially the same normal distribution (Fig. 4*B*, *right*).

Having found individual frequency components to be uncorrelated, we next characterized the amplitude distribution of spike discharge noise. To improve our estimate of the distribution, Fourier components from 0.3 to 20 Hz were combined on the grounds that their power spectral density was nearly constant (Fig. 3). Figure 5*A* plots the real versus imaginary amplitude of noise extracted at low temporal frequencies from the driven discharge of the two X cells in Fig. 2. The shape of the two histograms bordering the plots suggests that the scatter of points conforms to a two-dimensional circular Gaussian distribution. We confirmed this by converting from real and imaginary coordinates to amplitude and phase. For circularly distributed Gaussian noise, such a conversion produces a Rayleigh amplitude distribution (Watson 1990) and a uniform phase distribution. This held for every cell tested ($n = 9$). As an example, Fig. 5*B* plots the amplitude and phase distributions from 0.3-20 Hz (●) and 130–150 Hz (○), where noise power is also relatively constant, for the two X cells. As would be expected from Fig. 3, the 0.3 to 20 Hz distributions of the maintained and driven discharge noise were virtually identical as were the 130 to 150 Hz distributions for the ON-X cell. By contrast, the 130 to 150 Hz distributions of the maintained and driven noise differed greatly for the OFF-X cell owing to the stimulus-induced increase in high-frequency noise. Nevertheless, the amplitude distributions are all well fit by a Rayleigh function and the phase distributions are uniform ($R^2 > 0.99$). This result may seem counterintuitive given that spikes are all-or-nothing events, so we took the driven discharge noise on one trial and transformed it back to the time domain. In performing the inverse transformation, only Fourier compo-

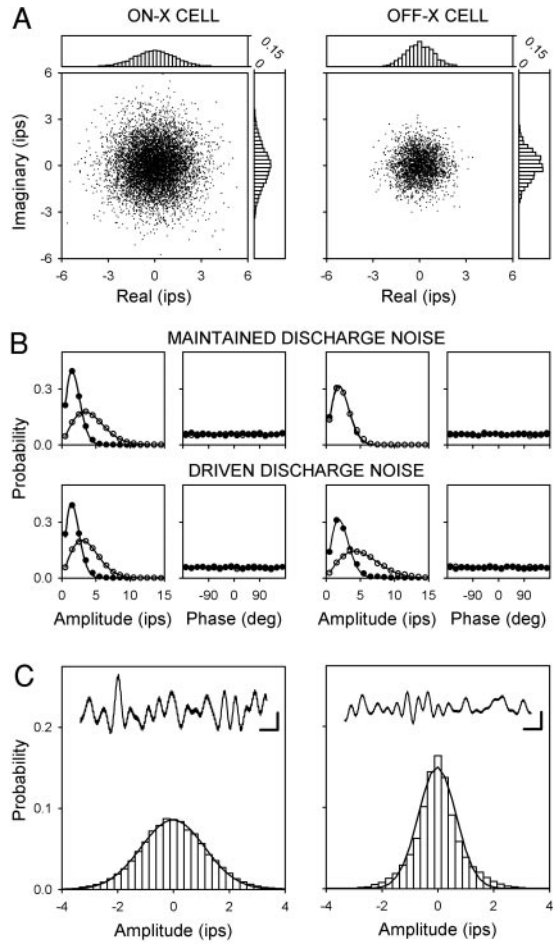

FIG. 5. Amplitude distribution of driven discharge noise. *A*: real vs. imaginary noise measurements from 0.3 to 20 Hz for the 2 X cells of Fig. 2. Histograms bordering the scatter plot give the probability distribution of real and imaginary amplitudes using a 0.25-imp/s bin width. *B*: noise magnitude and phase measurements from 0.3 to 20 Hz (●) and 130 to 150 Hz (○) for the maintained and driven discharge. —, the best fit of a Rayleigh function, $P(r) = (r/\sigma^2)\exp(-r^2/2\sigma^2)$, to the data. *C*: amplitude distribution in the time domain of spike discharge noise band-limited to 20 Hz. Bin width of the histogram is 0.25 imp/s. —, the best fit of a Gaussian function to the distribution ($\sigma = 1.1$ imp/s for the ON cell and 0.6 imp/s for the OFF cell). *Inset*: the temporal waveform of band-limited noise that was extracted from the response to a randomly modulated spot. Horizontal and vertical calibration bars are 0.1 s and 2 imp/s, respectively.

nents from −20 to 20 Hz were retained (all other components were assigned a value of 0), which amounts to band-pass filtering the spike train as the synapses of recipient neurons in the brain might do. Figure 5*C* illustrates that the temporal waveform of this band-limited noise is well approximated by a Gaussian amplitude distribution. Because the Fourier components of spike discharge noise are normally distributed and uncorrelated at low temporal frequencies, they would then be independent as well.

Noise is additive at low temporal frequencies

That visual stimulation had little effect on spike discharge noise over the range of 0.3–20 Hz suggests the noise at these temporal frequencies is additive as well. We quantitatively tested the notion of additivity by altering the contrast of the randomly modulated spot and measuring the signal and noise in the resulting spike trains. Figure 6 plots, for the ensemble of ganglion cells, the average contribution of signal (○) and noise (●) to the low-frequency power in their spot responses. The measurements were made by summing power spectral densities from −20 to 20 Hz and dividing by 300 (see METHODS). Spectral densities may be added because individual frequency components of spike discharge noise were found to be independent (Figs. 4 and 5). For all four cell types, the cumulative noise power <20 Hz showed a tendency to decrease with increasing contrast, presumably as a result of adaptation, saturation, or rectification within the retinal network. The slight reduction in noise level was, however, statistically significant only for ON cells (paired *t*-test between 0 and 100% contrast, $P < 0.05$) and paled in relation to the change in signal strength that accompanied it. At maximum spot contrast, for example, the cumulative signal power was 20–35 times greater than the noise power. Spike discharge noise thus added an essentially

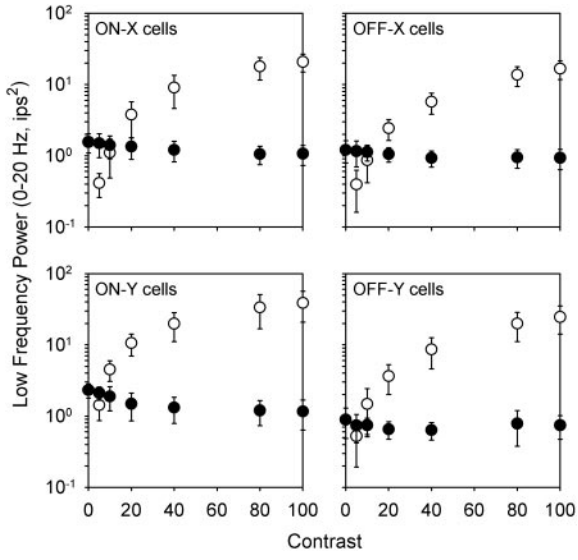

FIG. 6. Signal and noise contributions to the ganglion cell output. Plotted as a function of stimulus contrast is the low-frequency power in the response due to signal (○) and noise (●) averaged over the ensemble of ON and OFF X and Y cells. Signal and noise contributions were quantified by summing their respective power spectral densities from 0.3 to 20 and −0.3 to −20 Hz and dividing by 300. Error bars give SDs. Measurements are derived from 11 ON-X, 9 OFF-X, 9 ON-Y, and 13 OFF-Y cells.

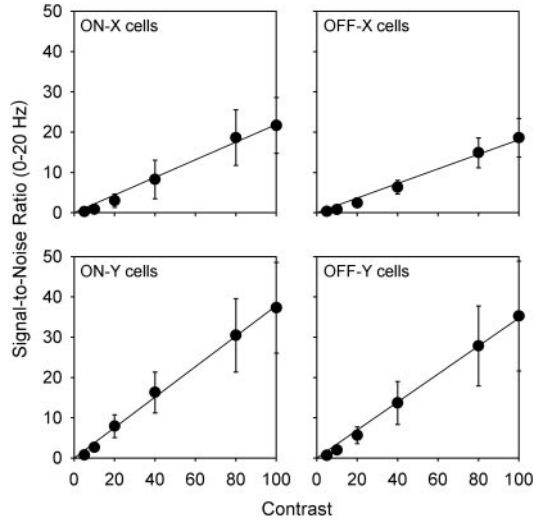

FIG. 7. Signal-to-noise ratio in the ganglion cell output. Plotted as a function of stimulus contrast is the cumulative signal-to-noise ratio from 0.3- to 20-Hz averaged over the ensemble of ON and OFF, X and Y cells in Fig. 6. The lines are linear (0-intercept) fits to the ensemble averages. The slopes of the lines are 0.22 and 0.18 for the ON- and OFF-X cells and 0.38 and 0.35 for the ON- and OFF-Y cells. The larger slope for Y cells reflects their higher contrast sensitivity. Error bars give SDs.

fixed amount of low frequency variance (~1 imp/s^2) to ganglion cell responses.

If only low-frequency transmission is considered, the discriminability of visual signals in the retinal output was found to increase linearly with stimulus strength (Fig. 7). That is to say, for a given type of ganglion cell, the average ratio of signal and noise power over the range of 0.3–20 Hz scaled in proportion to spot contrast ($R^2 > 0.98$). The slope of the best-fitting line, in terms of SNR per 1% contrast, was 0.22 for ON-X cells, 0.18 for OFF-X cells, 0.38 for ON-Y cells, and 0.35 for OFF-Y cells. The slopes for ON and OFF cells of the same cell-type (X or Y) were statistically indistinguishable, whereas those of X and Y cells were significantly different (Mann-Whitney test, $P \ll 0.01$ for the latter). That Y cells had nearly twice the contrast gain (i.e., slope) of X cells is consistent with previous measurements using sinusoidally modulated patterns (Derrington and Lennie 1982; Troy 1983). These contrast gain measures cannot be directly compared with the reported contrast sensitivities of the cells, however, because our stimulus contained more than one sinusoidal component.

Modeling noise in ganglion cell spike trains

Modeling studies have shown that artificial spike trains having similar interval statistics as the maintained discharge of retinal ganglion cells can be created using an integrate-and-fire coding mechanism (Levine 1992). We found that such a simple encoder could also capture the observed properties of the driven discharge reasonably well (Passaglia and Troy 2004). Figure 8*A* displays a block diagram of the model. It assumes that retinal noise is additive, white, and Gaussian distributed in amplitude and arises largely after the network has transformed the visual stimulus into the signal input to the ganglion cell spike generator. The spike generator integrates the two variables and, when the integral crosses a threshold level, it fires a

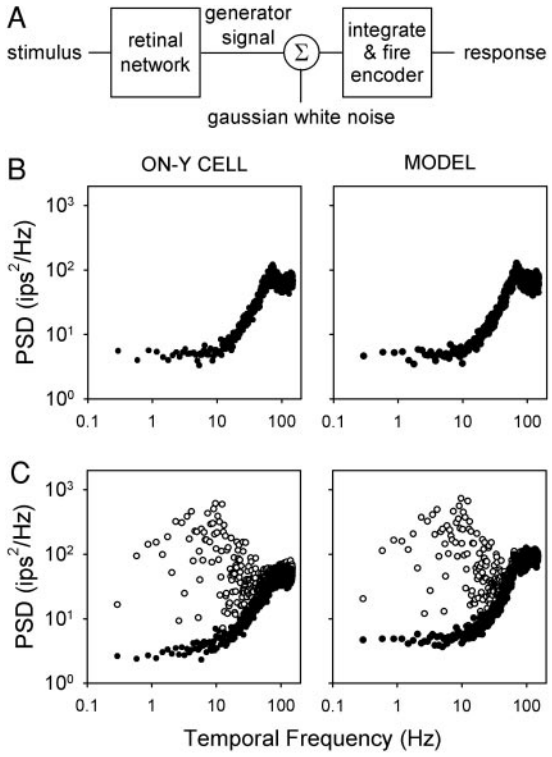

FIG. 8. Simulating ganglion cell spike trains. *A*: artificial retinal responses to a randomly modulated spot stimulus were produced by adding Gaussian white noise to the deterministic signal generated by the retinal network and passing the signal and noise through an integrate-and-fire encoder. The generator signal was defined by the average response of a ganglion cell to a repeated random binary sequence of high contrast (e.g., histograms in Fig. 2*B*). This model has 3 parameters: α, which sets the mean spike rate in the absence of a stimulus; β, which sets the contrast gain; and γ, which sets the SD of the discharge noise. These parameters were varied to qualitatively match the power spectra of the maintained and driven discharge of a given ganglion cell. *B*: power spectra of the maintained discharge of an ON-Y cell and a model of the cell. *C*: power spectra of the average driven response (○) and the driven discharge noise (●) of the ON-Y cell and the model. This simple model can reproduce our basic finding that, even when vigorously driven, the noise in the maintained and driven discharge can be the same at low temporal frequencies.

spike and resets to zero. The response of the model $r_{LN}(t)$ to an arbitrary generator signal is given by

$$r_m(t) = \begin{cases} 0, \Sigma\Delta t[\alpha + \beta x(t) + \gamma n(t)] < 1 \\ 1, \text{otherwise} \end{cases} \quad (4)$$

where Δt is the model time step (1/600 s), α sets the mean spike rate of the model neuron in the absence of a stimulus, β is the contrast gain of the model neuron, $x(t)$ is the average response modulation of a ganglion cell to the random binary spot sequence, $n(t)$ is Gaussian noise of unit variance, and is the SD of the noise. Because of rectification, refractoriness, and adaptation of the spiking mechanism $x(t)$ might not match the actual generator signal of the cell, but it should have comparable temporal dynamics. To simulate the maintained discharge of a given cell (i.e., $\beta = 0$), we fixed α to produce the mean spike rate and adjusted γ to give a similar variability of spike discharge. Figure 8*B* shows for the ON-Y cell in Fig. 3 that the model closely reproduces the power spectrum of the maintained discharge. Without altering γ, we then varied β to simulate the driven discharge of the cell to repeated presentation of a randomly modulated spot of different contrasts (see histograms in Fig. 2*B*). Figure 8C (○) shows that, for the appropriate gain setting, the power spectrum of model spike trains resembles that of the ON-Y cell. We then extracted the driven discharge noise from model spike trains as we did with retinal spike trains. Like the ON-Y cell, the maintained and driven noise spectra of the model were nearly identical (compare ● in Fig. 8, *B* and *C*), especially at temporal frequencies less than ~20 Hz. Other ON-cell models yielded similar results ($n = 5$). Because signal rectification by the spiking mechanism was included in the model, we infer that the slight reduction in low-frequency noise seen in ON cells at high contrast is due to some other nonlinearity.

DISCUSSION

Our main finding is that variability in the spike trains of retinal ganglion cells during constant and dynamic stimulation can exhibit different properties depending on the time interval of measurement. If analyzed on a slow time scale in which only frequency components from 0.3 to 20 Hz are included, spike discharge noise is independent of stimulus contrast and thus additive. The noise also exhibits other interesting properties; namely, it has minimal variance, the variance is uniformly distributed over frequency, and individual frequency components are independent and Gaussian distributed in amplitude. Moreover, for these temporal frequencies, the signal-to-noise ratio of the retinal output is linear with stimulus contrast. Such noise characteristics make the visual signal simple to decode. On the other hand, if variability in ganglion cell spike trains is analyzed on a fine time scale so that frequency components greater than ~20 Hz are included, spike discharge noise shows a strong dependence on stimulus contrast and thus appears multiplicative. The stimulus dependence arises because noise power spectral density increases at high temporal frequencies to a plateau level that is determined by the mean spike rate, which usually varies with contrast. Our results do not address whether visual cortical cells make use of information present at high temporal frequencies in retinal spike train but they do indicate that distinguishing signal from noise in this regime is more complicated.

Our findings can explain a seemingly paradoxical result in the literature. Several studies have shown that the variance in ganglion cell spike rate to a constant or dynamic stimulus depends on the mean spike rate (e.g., Berry et al. 1997; Frishman and Levine 1983; Kara et al. 2000), which implies that noise is multiplicative. Yet other studies have shown that the variance in amplitude of ganglion cell responses to a periodic stimulus is independent of the mean response amplitude (e.g., Croner et al. 1993; Reich et al. 1997; van Dijk and Ringo 1987), which implies that noise is additive. How can this be? The two results follow from our findings because the former studies typically used interval or spike-count statistics to analyze spike trains. Interval-based statistics implicitly span a range of time scales (from the shortest to the longest interspike interval) and thus include the high-frequency range where noise is multiplicative. And spike-count statistics like the Fano factor (i.e., variance-to-mean spike count) depend on the time window over which spikes are counted, which is often short in duration to evaluate spike count precision. By contrast, the latter studies analyzed only the component of spike discharge noise at the frequency of visual stimulation and this

frequency component was naturally <20 Hz to evoke a strong response from ganglion cells. For example, it may be seen that Fig. 6 bears much resemblance to results reported by Croner et al. (1993). This resemblance is due to our restricting the noise variance measurement to frequency components <20 Hz. If higher frequency components are included (Fig. 9), noise variance depends strongly on stimulus contrast. Hence based on our results we suspect that if Croner et al. (1993) had used a stimulus frequency >20 Hz or defined noise to be the residual error in their sinusoidal fit (which includes all noise frequency components) instead of the variance in fundamental response amplitude (which involves just one component), they would have obtained a different result.

Our findings also suggest that spike discharge noise might exhibit additive properties in other areas of the brain, even those areas where it is commonly thought to be multiplicative. For example, it is widely reported that the number of spikes fired by visual cortical cells in response to a visual stimulus is highly variable and that the amount of variability increases with stimulus contrast (Dean 1981; Shadlen and Newsome 1998; Tolhurst et al. 1983). The dependence on contrast indicates that cortical noise, on the whole, is multiplicative. But as we have shown here for retinal ganglion cells, individual frequency components of the noise could still be additive. Like visual cortical cells in the preceding studies, the discharge noise of OFF ganglion cells increases with contrast if the total variance in their spike trains is measured (Fig. 9). It is only when the portion of the variance less than ~20 Hz (i.e., counting windows >25 ms) is considered that the noise appears independent of the encoded signal. Interestingly, two studies have characterized the response variability of cells in middle temporal (Buračas et al. 1998) and primary visual cortex (Kara et al. 2000) as a function of the time scale of analysis, and they both found that lengthening the analysis window greatly reduced the variance-to-mean spike count ratio. Moreover, in the latter study, the ratio was constant for windows >25–50 ms, which suggests that the power spectrum of cortical noise could also be minimal and constant <20 Hz like that of retinal noise (Fig. 3) and geniculate noise (Mukherkee and Kaplan 1998). There is thus indirect evidence that noise in the output of lateral geniculate and primary visual cortical cells might be additive at low temporal frequencies as well.

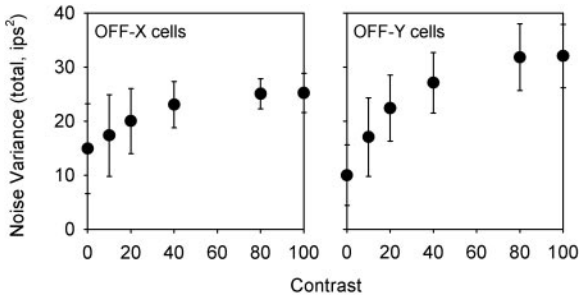

FIG. 9. Total discharge noise in OFF ganglion cells increases with contrast. Noise variance was determined by summing the noise power spectra of OFF-X and OFF -Y cells over all temporal frequencies except 0 Hz. This is equivalent to measuring the variance directly from the driven noise records. Error bars give SDs. Measurements are derived from the same 9 OFF-X and 13 OFF-Y cells of Fig. 6.

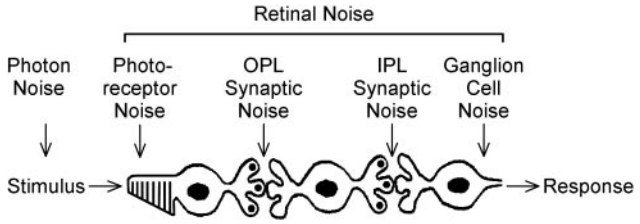

FIG. 10. Possible sources of noise in the retinal output. Under scotopic conditions, spike discharge noise is due primarily to photon and photoreceptor noise (Barlow et al. 1971). Under photopic conditions noise arising later in the retinal pathway may become significant as a result of light adaptation. This is because noise at the retinal input traverses the same retinal nonlinearities that act on the signal and would thus get attenuated as the retina adapts, whereas noise at the retinal output would not. IPL, inner plexiform layer. OPL, outer plexiform layer.

Implications for retinal noise

The retinal network employs a variety of mechanisms to transform the visual stimulus into the signal that ganglion cells transmit to the brain. These mechanisms often behave linearly for weak signals and nonlinearly for strong signals. Because photon noise accompanying the visual stimulus and neural noise originating early within the retinal network must pass through the same transformations (Fig. 10), it is expected that spike discharge noise would depend strongly on signal strength and not behave additively. That the maintained and driven noise spectra differed little for ON cells and, at low temporal frequencies, little for OFF cells is thus surprising. It suggests that much of the noise at this photopic light level arose after retinal nonlinearities had already operated on the signal encoded in the spike train. Such a noise source presumably resides late in the retinal pathway, at bipolar-to-ganglion cell synapses (Freed 2000), or perhaps within ganglion cells themselves (Croner et al. 1993; Schellart and Spekreijse 1973). That the spike encoder could be noisy is supported by a recent study that used a detailed computational model of a cat X cell to examine the effect of various sources of retinal noise on spike timing precision (van Rossom et al. 2003). By turning off noise sources individually in the model, they found that up to half the variability in spike timing could be attributed to membrane channel noise in ganglion cells. Why noise should predominately arise late in the retinal pathway under photopic conditions, but not under scotopic conditions (Barlow et al. 1971), is presently unclear though light adaptation is surely involved.

Implications for visual information transmission

The standard procedure for quantifying the information transmission rate of a neuron is to directly measure the probability distribution of its responses to a given stimulus (de Ruyter van Steveninck et al. 1997; McClurkin et al. 1991; Reinagel and Reid 2000). A major drawback of this direct approach is that large amounts of data are required to accurately measure the probability distribution, which greatly limits the variety of stimuli that can be investigated in an experiment. If, however, the response probability distribution can be approximated by a Gaussian function the variance of which is given by the addition of signal and noise, neural information transmission can be examined more efficiently by measuring signal-to-noise ratios (Borst and Theunissen 1999; Rieke et al.

1997). For an additive Gaussian noise channel, the information rate I is given by

$$I = \delta f \sum_f \log_2 [1 + \mathrm{SNR}(f)] \quad (5)$$

where SNR(f) is the ratio of signal-to-noise power spectral density at temporal frequency f and δf is the spectral bin width (~0.3 Hz in our study). Table 1 lists the five conditions that must be met for *Eq. 5* to correctly estimate the information rate. Although this equation is not generally valid because noise behaves multiplicatively at fine time scales, as others have argued (Cecchi et al. 2000), our results indicate that it would still apply to low-frequency components of retinal spike trains where the conditions of additivity, frequency independence, and Gaussian-distributed amplitudes hold. This means that, with the appropriate choice of stimulus so that the encoded signal satisfies its conditions as well, signal-to-noise ratios should provide an accurate estimate of the information transmission rate of a retinal ganglion cell over the range of 0.3–20 Hz. Using *Eq. 5*, we estimate the information rate over this frequency range to be 51.5 ± 5.1 bits/s (bps) for the ensemble of ON-X cells, 41.1 ± 3.2 bps for OFF-X cells, 47.3 ± 2.8 bps for ON-Y cells, and 43.6 ± 4.3 bps for OFF-Y cells for a 100%-contrast randomly modulated spot matched in size to the receptive field center. Although these transmission rates are substantial, the total information rate of the cells for this stimulus is ~100 bps (Passaglia and Troy 2004), which begs the question of what information is actually important to the brain.

In the primary visual cortex, it so happens that cells respond best to precisely the range of stimulus frequencies where noise in the retinal output is additive, white, and Gaussian. Figure 11 plots the driven discharge noise spectrum of the ON-X cell in Fig. 3 together with the contrast sensitivity measurements of Movshon et al. (1978) for six cells in area 17 of the cat visual cortex. Similar temporal tuning curves have been reported by other studies of cells in the input layers of the cat and monkey primary visual cortices (Bisti et al. 1985; Foster et al. 1985; Geisler and Albrecht 1997; O'Keefe et al. 1998; but see Hawken et al. 1996). The curves show that visual cortical cells are maximally sensitive to stimulus modulations in the range of 2–8 Hz and give little or no response to modulation frequencies >20 Hz, where noise in ganglion cell spike trains is maximal and strongly dependent on the stimulus. The apparent matching of the cortical receiver with the signal and noise characteristics of the retinal transmitter to yield an information channel in which signal-to-noise ratio would scale linearly with stimulus contrast (Fig. 7) suggests that this region of the brain ignores the fine structure of ganglion cell spike trains. The suggestion is further strengthened by psychophysical studies which indicate that cats barely see spatial patterns modulated faster than 20 Hz (Blake and Camisa 1977). Hence, noise in the retinal output appears to be additive, white, and Gaussian from the perspective of primary visual cortical cells and the information conveyed to these cells can be estimated from signal-to-noise ratios. This notion might not apply to other regions of the brain where the precise patterning of ganglion cell spikes could be meaningful.

TABLE 1. *Conditions for estimating information transmission using signal-to-noise ratios*

Amplitude distribution of signal is Gaussian
Frequency components of signal are independent
Amplitude distribution of noise is Gaussian
Frequency components of noise are independent
Signal and noise combine additively

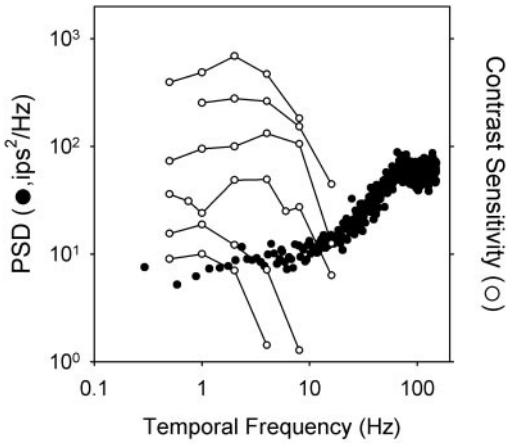

FIG. 11. Relation of retinal noise measurements to reported temporal tuning curves of visual cortical cells. ○, the temporal contrast sensitivity measurements of 6 cells in area 17 of cat visual cortex from Fig. 8 of Movshon et al. (1978). The contrast sensitivity curves have been displaced vertically for clarity. ●, the driven discharge noise of the ON-X cell in Fig. 3 for purpose of comparison.

Implications for decoding neural spike trains

There are many views of how neural spike trains convey information. These views are often grouped according to the importance they place on the rate and the precise timing of spikes (Passaglia et al. 1997; Rieke et al. 1997; Shadlen and Newsome 1994; Theunissen and Miller 1995; Victor 1999), although the difference between rate and temporal coding is not always clear. Power spectral analysis addresses both coding strategies to some extent because it measures variability in spike trains across a range of time scales. Our results indicate that, while a strong stimulus can evoke spikes with high temporal precision (<5-ms jitter for some retinal spikes), response reproducibility does not necessarily imply temporal coding any more than rate coding because noise in the retinal output is additive and minimal over much of the signaling range of retinal ganglion cells and because noise is the same or even greater for the driven discharge than for the maintained discharge. That spike discharge noise could be similar for a constant and dynamic stimulus has also been reported for visual neurons in the fly brain (Warzecha and Egelhaaf 1999; Warzecha et al. 2000; but see de Ruyter van Steveninck et al. 1997). Given the relatively low level of noise at frequencies to which ganglion cells respond best, it may thus be expected that a strong stimulus like a randomly modulated high-contrast spot would elicit a highly reproducible train of spikes (Knight 1972). Hence, for temporal coding to differ from rate coding, even when signal-to-noise ratio is high, the precise patterning of spikes dictated by the linear drive to a neuron must be altered by nonlinearities associated with the spiking mechanism such as spike threshold and spike refractoriness (Passaglia and Troy 2004; Reich et al. 1998). If these alterations are distinguishable from noise, the spike patterns could then convey information that would be unrecoverable from spike rate

alone (Berry and Meister 1998). While power spectral analysis does not address the possibility of such high-order correlations in the spike train, they do not appear to have adversely affected our results because individual frequency components of the driven discharge noise of ganglion cells were Gaussian distributed in amplitude and uncorrelated even for high-contrast spots (Fig. 4). And since the spike rate already conveys a significant amount of information (Passaglia and Troy 2004) and spike discharge noise is greater and multiplicative at high temporal frequencies, the need to decode information embedded in precise spike patterns is uncertain.

ACKNOWLEDGMENTS

We thank Dr. Misha Vorobyev for suggestions on data analysis and Drs. Christina Enroth-Cugell, Jonathan Demb, Steven DeVries, David Ferster, Sara Solla, and Misha Vorobyev for helpful comments on the manuscript.

GRANTS

This research was supported by National Eye Institute Grants F32-EY-06908 and R01-EY-06669.

REFERENCES

Bair W and Koch C. Temporal precision of spike trains in extrastriate cortex of the behaving macaque monkey. *Neural Comput* 8: 1185–1202, 1996.

Barlow HB and Levick WR. Changes in the maintained discharge with adaptation level in the cat retina. *J Physiol* 202: 669–718, 1969.

Barlow HB, Levick WR, and Yoon M. Responses to single quanta of light in retinal ganglion cells of the cat. *Vision Res Suppl* 3: 87–101, 1971.

Berry MJ and Meister M. Refractoriness and neural precision. *J Neurosci* 18: 2200–2211, 1998.

Berry MJ, Warland DK, and Meister M. The structure and precision of retinal spike trains. *Proc Natl Acad Sci USA* 94: 5411–5416, 1997.

Bialek W, Rieke F, de Ruyter van Steveninck RR, and Warland D. Reading a neural code. *Science* 252: 1854–1857, 1991.

Bisti S, Carmignoto G, Galli L, and Maffei L. Spatial frequency characteristics of neurons of area 18 in the cat: dependence on the velocity of the visual stimulus. *J Physiol* 359: 259–268, 1985.

Blake R and Camisa JM. Temporal aspects of spatial vision in the cat. *Exp Brain Res* 28: 325–333, 1977.

Borst A and Theunissen FE. Information theory and neural coding. *Nat Neurosci* 2: 947–957, 1999.

Buračas GT, Zador AM, deWeese MR, and Albright TD. Efficient discrimination of temporal patterns by motion-sensitive neurons in primate visual cortex. *Neuron* 20: 959–969, 1998.

Bryant HL and Segundo JP. Spike initiation by transmembrane current: a white-noise analysis. *J Physiol* 260: 279–314, 1976.

Cecchi GA, Sigman M, Alonso J-M, Martinez L, Chialvo DR, and Magnasco MO. Noise in neurons is message dependent. *Proc Natl Acad Sci USA* 97: 5557–5561, 2000.

Croner LJ, Purpura K, and Kaplan E. Response variability in retinal ganglion cells of primates. *Proc Natl Acad Sci USA* 90: 8128–8130, 1993.

Dacey DM. Parallel pathways for spectral coding in primate retina. *Annu Rev Neurosci* 23: 743–75, 2000.

Dan Y, Alonso J-M, Usrey WM, and Reid RC. Coding of visual information by precisely correlated spikes in the lateral geniculate nucleus. *Nat Neurosci* 1: 501–507, 1998.

Dean AF. The variability of discharge of simple cells in the cat striate cortex. *Exp Brain Res* 44: 437–440, 1981.

Derrington AM and Lennie P. The influence of temporal frequency and adaptation level on receptive field organization of retinal ganglion cells in cat. *J Physiol* 333: 343–366, 1982.

de Ruyter van Steveninck RR, Lewen GD, Strong SP, Koberle R, and Bialek W. Reproducibility and variability in neural spike trains. *Science* 275: 1805–1808, 1997.

Enroth-Cugell C and Robson JG. The contrast sensitivity of retinal ganglion cells of the cat. *J Physiol* 187: 517–552, 1966.

Foster KH, Gaska JP, Nagler M, and Pollen DA. Spatial and temporal frequency selectivity of neurons in visual cortical areas V1 and V2 of the macaque monkey. *J Physiol* 365: 331–363, 1985.

Freed MA. Rate of quantal excitation to a retinal ganglion cell evoked by sensory input. *J Neurophysiol* 83: 2956–2966, 2000.

Frishman LJ, Freeman AW, Troy JB, Schweitzer-Tong DE, and Enroth-Cugell C. Spatiotemporal frequency response of cat retinal ganglion cells. *J Gen Physiol* 89: 599–628, 1987.

Frishman LJ and Levine MW. Statistics of the maintained discharge of cat retinal ganglion cells. *J Physiol* 339: 475–494, 1983.

Geisler WS and Albrecht DG. Visual cortex neurons in monkeys and cats: detection, discrimination, and identification. *Vis Neurosci* 14: 897–919, 1997.

Hawken MJ, Shapley RM, and Grossof DH. Temporal-frequency selectivity in monkey visual cortex. *Vis Neurosci* 13: 477–492, 1996.

Hecht S, Schlaer S, and Pirenne MH. Energy, quanta, and vision. *J Gen Physiol* 25: 819–840, 1942.

Hochstein S and Shapley RM. Quantitative analysis of retinal ganglion cell classifications. *J Physiol* 262: 237–264, 1976.

Hubel DH and Wiesel TN. Receptive fields, binocular interaction and functional architecture in the cat's visual cortex. *J Physiol* 160: 106–154, 1962.

Kara P, Reinagel P, and Reid RC. Low response variability in simultaneously recorded retinal, thalamic, and cortical neurons. *Neuron* 27: 635–646, 2000.

Keat J, Reinagel P, Reid RC, and Meister M. Predicting every spike: a model for the responses of visual neurons. *Neuron* 30: 803–817, 2001.

Knight BW. Dynamics of encoding in a population of neurons. *J Gen Physiol* 59: 734–766, 1972.

Kuffler SW. Discharge patterns and functional organization of mammalian retina. *J Neurophysiol* 16: 37–68, 1953.

Kuffler SW, Fitzhugh R, and Barlow HB. Maintained activity in the cat's retina in light and darkness. *J Gen Physiol* 40: 683–702, 1957.

Lennie P. Parallel visual pathways: a review. *Vision Res* 20: 561–594, 1980.

Levine MW. Modeling the variability of firing rate of retinal ganglion cells. *Math Biosci* 112: 225–242, 1992.

Levine MW. Variablity of responses to sinusoidal modulation. *Vis Neurosci* 11: 155–163, 1994.

Liu RC, Tzonev S, Rebrik S, and Miller KD. Variability and information in a neural code of the cat lateral geniculate nucleus. *J Neurophysiol* 86: 2789–2806, 2001.

Lowen SB, Ozaki T, Kaplan E, Saleh BEA, and Teich MC. Fractal features of dark, maintained, and driven neural discharge in the cat visual system. *Methods* 24: 377–394, 2001.

Mainen ZF and Sejnowski TJ. Reliability of spike timing in neocortical neurons. *Science* 268: 1503–1506, 1995.

McClurkin JW, Gawne TJ, Optican LM, and Richmond BJ. Lateral geniculate neurons in behaving primates. II. Encoding of visual information in the temporal shape of the response. *J Neurophysiol* 66: 794–808, 1991.

Movshon JA, Thompson ID, and Tolhurst DJ. Spatial and temporal contrast sensitivity of neurons in areas 17 and 18 of the cat's visual cortex. *J Physiol* 283: 101–120, 1978.

Mukherjee P and Kaplan E. The maintained discharge of neurons in the cat lateral geniculate nucleus: spectral analysis and computational modeling. *Vis Neurosci* 15: 529–539, 1998.

Nirenberg S, Carcieri SM, Jacobs AL, and Latham PE. Retinal ganglion cells act largely as independent encoders. *Nature* 411: 698–701, 2001.

Nowak LG, Sanchez-Vives MV, and McCormick DA. Influence of low and high frequency inputs on spike timing in visual cortical neurons. *Cereb Cortex* 7: 487–501, 1997.

O'Keefe LP, Levitt JB, Kiper DC, Shapley RM, and Movshon JA. Functional organization of owl monkey lateral geniculate nucleus and visual cortex. *J Neurophysiol* 80: 594–609, 1998.

Passaglia C, Dodge F, Herzog E, Jackson S, and Barlow R. Deciphering a neural code for vision. *Proc Natl Acad Sci USA* 94: 12649–12654, 1997.

Passaglia CL and Troy JB. Information transmission rates of cat retinal ganglion cells. *J Neurophysiol* 91: 1217–1229, 2004.

Reich DS, Victor JD, and Knight BW. The power ratio and the interval map: spiking models and extracellular recordings. *J Neurosci* 18: 10090–10104, 1998.

Reich DS, Victor J, Knight BW, Ozaki T, and Kaplan E. Response variability and timing precision of neuronal spike trains in vivo. *J Neurophysiol* 77: 2836–2841, 1997.

Reinagel P and Reid RC. Temporal coding of visual information in the thalamus. *J Neurosci* 20: 5392–5400, 2000.

Rieke F, Warland D, de Ruyter van Steveninck RR, and Bialek W. *Spikes: Exploring the Neural Code.* Cambridge, MA: MIT Press, 1997.

Rodieck RW. Maintained activity of cat retinal ganglion cells. *J Neurophysiol* 30: 1043–1071, 1967.

Rüttiger L, Lee B, and Sun H. Transient cells can be neurometrically sustained: the positional accuracy of retinal signals to moving targets. *J Vision* 2: 232–242, 2002.

Schellart NAM and Spekreijse H. Origin of the stochastic nature of ganglion cell activity in isolated goldfish retina. *Vision Res* 13: 337–344, 1973.

Schiller PH. The ON and OFF channels of the visual system. *Trends Neurosci* 15: 86–92, 1992.

Schneeweis DM and Schnapf JL. The photovoltage of macaque cone photoreceptors: adaptation, noise, and kinetics. *J Neurosci* 19: 1203–1216, 1999.

Shadlen MN and Newsome WT. Noise, neural codes and cortical organization. *Curr Opin Neurobiol* 4: 569–579, 1994.

Shadlen MN and Newsome WT. The variable discharge of cortical neurons: implications for connectivity, computation, and information coding. *J Neurosci* 18: 3870–3896, 1998.

Shapley R and Enroth-Cugell C. Visual adaptation and retinal gain controls. *Prog Retinal Res* 3: 263–346, 1984.

Strong SP, Koberle R, de Ruyter van Steveninck RR, and Bialek W. Entropy and information in neural spike trains. *Phys Rev Lett* 80: 197–200, 1998.

Teich MC, Heneghan C, Lowen SB, Ozaki T, and Kaplan E. Fractal character of the neural spike train in the visual system of the cat. *J Opt Soc Am A* 14: 529–546, 1997.

Theunissen FE and Miller JP. Temporal encoding in nervous systems: a rigorous definition. *J Comp Neurosci* 2: 149–162, 1995.

Tolhurst DF, Movshon JA, and Dean AF. The statistical reliability of signals in single neurons in cat and monkey visual cortex. *Vision Res* 23: 775–785, 1983.

Troy JB. Spatial contrast sensitivities of X and Y type neurons in the cat's dorsal lateral geniculate nucleus. *J Physiol* 344: 399–417, 1983.

Troy JB and Lee BB. Steady discharges of macaque retinal ganglion cells. *Vis Neurosci* 11: 111–118, 1994.

Troy JB and Robson JG. Steady discharges of X and Y retinal ganglion cells of cat under photopic illumination. *Vis Neurosci* 9: 535–553, 1992.

van Dijk BW and Ringo JL. The variation in the light responses of carp retinal ganlgion cells is independent of response amplitude. *Vision Res* 27: 493–497, 1987.

van Rossum MCW, O'Brien BJ, and Smith RG. Effects of noise on the spike timing precision of retinal ganglion cells. *J Neurophysiol* 89: 2406–2419, 2003.

Victor JD. Temporal aspects of neural coding in the retina and lateral geniculate. *Network* 10: R1–R66, 1999.

Warzecha A-K and Egelhaaf M. Variability in spike trains during constant and dynamic stimulation. *Science* 283: 1927–1930, 1999.

Warzecha A-K, Kretzberg J, and Egelhaaf M. Reliability of a fly motion-sensitive neuron depends on stimulus parameters. *J Neurosci* 20: 8886–8896, 2000.

Watson AB. Gain, noise, and contrast sensitivity of linear visual neurons. *Vis Neurosci* 4: 147–157, 1990.